

1 ***Ehrlichia ruminantium* uses its transmembrane protein Ape to adhere to**  
2 **host bovine aortic endothelial cells**

3

4 Valérie Pinarello<sup>1,2#</sup>, Elena Bencurova<sup>3</sup>, Isabel Marcelino<sup>4</sup>, Olivier Gros<sup>5</sup>, Carinne Puech<sup>2</sup>,  
5 Mangesh Bhide<sup>3,6</sup>, Nathalie Vachieri<sup>2</sup> and Damien F. Meyer<sup>1,2\*</sup>.

6

7 <sup>1</sup>CIRAD, UMR ASTRE, F-97170 Petit-Bourg, Guadeloupe, France

8 <sup>2</sup>ASTRE, CIRAD, INRA, Univ Montpellier, Montpellier, France

9 <sup>3</sup> Laboratory of biomedical microbiology and immunology, University of veterinary medicine  
10 and pharmacy in Kosice, Komenskeho 73, Kosice, Slovakia

11 <sup>4</sup> Institut Pasteur de la Guadeloupe, 97183 Les Abymes Cedex, Guadeloupe, France

12 <sup>5</sup> Institut de Systématique, Évolution, Biodiversité (ISYEB), Muséum national d'Histoire  
13 naturelle, CNRS, Sorbonne Université, EPHE, Université des Antilles  
14 Campus de Fouillole, 97110 Pointe-à-Pitre, France

15 <sup>6</sup> Institute of neuroimmunology, Slovak academy of sciences, Bratislava, Dubravska cesta  
16 9, Slovakia

17

18 # present address: CIRAD, UMR ASTRE, Harare, Zimbabwe

19 \*Email: [damien.meyer@cirad.fr](mailto:damien.meyer@cirad.fr)

20

## 21 **Abstract**

22 *Ehrlichia ruminantium* is an obligate intracellular bacterium, transmitted by ticks of the  
23 genus *Amblyomma* and responsible for heartwater, a disease of domestic and wild  
24 ruminants. High genetic diversity of *E. ruminantium* strains hampers the development of an  
25 effective vaccine against all strains present in the field. In order to develop strategies for  
26 the control of heartwater through both vaccine and alternative therapeutic approaches, it is  
27 important to first gain a better understanding of the early interaction of *E. ruminantium* and  
28 its host cell. Particularly, the mechanisms associated with bacterial adhesion remain to  
29 elucidate. Herein, we studied the role of *E. ruminantium* membrane protein  
30 ERGA\_CDS\_01230 (UniProt Q5FFA9), a probable iron transporter, in the adhesion  
31 process to host bovine aortic endothelial cells (BAEC). The recombinant version of the  
32 protein ERGA\_CDS\_01230, successfully produced in the *Leishmania tarentolae* system, is  
33 O-glycosylated. Following *in vitro* culture of *E. ruminantium* in BAEC, the expression of  
34 CDS ERGA\_CDS\_01230 peaks at the extracellular infectious elementary body stages.  
35 This result suggest the likely involvement of ERGA\_CDS\_01230, named hereafter Ape for  
36 Adhesion protein of E*hrlichia*, in the early interaction of *E. ruminantium* with its host cells.  
37 We showed using flow cytometry and scanning electron microscopy that beads coated  
38 with recombinant ERGA\_CDS\_01230 (rApe) adheres to BAEC. In addition, we also  
39 observed that rApe interacts with proteins of the cell lysate, membrane and organelle  
40 fractions. Additionally, enzymatic treatment degrading dermatan and chondroitin sulfates  
41 on the surface of BAEC is associated with a 50% reduction in the number of bacteria in the  
42 host cell after a development cycle, indicating that glycosaminoglycans seem to play a role  
43 in the adhesion of *E. ruminantium* to the host cell. Finally, Ape induces a humoral  
44 response in vaccinated animals. Globally, our work identifying the role of Ape in *E.*  
45 *ruminantium* adhesion to host cells makes it a gold vaccine candidate and represents a  
46 first step toward the understanding of the mechanisms of cell invasion by *E. ruminantium*.

47

## 48 Introduction

49 *Ehrlichia ruminantium* is an obligate intracellular Gram-negative bacterium responsible for  
50 the fatal and neglected heartwater disease of domestic and wild ruminants (Allsopp, 2010).  
51 This bacterium belongs to the *Anaplasmataceae* family in the order *Rickettsiales* that  
52 includes many pathogens and symbionts of veterinary and public health importance  
53 (Moumene and Meyer, 2015). *E. ruminantium* is transmitted by ticks of the genus  
54 *Amblyomma* in the tropical and sub-Saharan areas, as well as in the Caribbean islands,  
55 and constitutes a major threat for the American livestock industries since a suitable tick  
56 vector is already present in the American mainland and potential introduction of infected *A.*  
57 *variegatum* through migratory birds or uncontrolled movement of animals from Caribbean  
58 could occur (Deem, 1998; Kasari et al., 2010). The disease is also a major obstacle to the  
59 introduction of animals from heartwater-free to heartwater-infected areas into sub-Saharan  
60 Africa and thus restrains the breeding to upgrade local stocks (Allsopp, 2010). The small  
61 genome of *E. ruminantium* (1.5 Mb) shows an unique process of contraction/expansion in  
62 non-coding regions and targeted at tandem repeats (Frutos et al., 2006). This ongoing  
63 genome plasticity, associated with a high genetic diversity, suggests a capacity of  
64 adaptation upon exposure to a novel environment but could also explain the low field  
65 efficacy of available vaccines (Cangi et al., 2016).

66 After adhesion and entry of infectious elementary bodies into host cells, *E. ruminantium*  
67 replicates by binary fission of reticulated bodies into an intracellular vacuole bounded by a  
68 lipid bilayer membrane derived from the eukaryotic host endothelial cell membrane  
69 (Dumler et al., 2001). *Ehrlichia* spp. have evolved sophisticated mechanisms to invade and  
70 multiply in host tissues by hijacking/subverting host cell processes ranging from host  
71 signaling, modulation of vesicular traffic, protection from oxidative burst, acquisition of  
72 nutrients, and control of innate immune activation (Moumene and Meyer, 2015). Notably,  
73 *E. chaffeensis* secretes the type IV effector Etf-1 to induce autophagy and capture  
74 nutrients, whereas it uses Etf-2 to delay endosome maturation to avoid phagolysosomal  
75 fusion for the benefit of bacterial replication (Lin et al., 2016; Yan et al., 2018). Moreover,  
76 recent work identified that *E. chaffeensis* uses EtpE invasin to enter mammalian cells via  
77 the binding to its receptor DNaseX, a glycosylphosphatidylinositol-anchored cell surface  
78 receptor (Mohan Kumar et al., 2013). That receptor-triggered entry simultaneously blocks  
79 the generation of reactive oxygen species (ROS) by host monocytes and macrophages  
80 (Teymournejad et al., 2017).

81 Due to the lack of some key metabolic genes that are required for host-free living and  
82 similarly to what observed for other intracellular bacteria, entry into the eukaryotic host  
83 cells is crucial for *E. ruminantium* to sustain its life and disseminate (Pizarro-Cerda and  
84 Cossart, 2006) ; (Frutos et al., 2007). Computational studies allowed the prediction of type  
85 IV effectors for *E. ruminantium* (Noroy et al., 2019) that remain to be fully characterized but  
86 detailed mechanisms of adhesion and entry are still unknown. These processes can be  
87 active or passive depending on the pathogen. *E. ruminantium* could either inject a type IV  
88 effector across the host cell membrane to trigger actin rearrangement and pathogen  
89 phagocytosis such as *Bartonella henselae* (Truttmann et al., 2011). An another option is  
90 the use of homologous system of *E. chaffeensis* invasion/receptor pair (Mohan Kumar et  
91 al., 2013) or an outer membrane protein of the OmpA family that actively trigger  
92 internalization as was observed in *Coxiella burnettii* (Martinez et al., 2014).

93 Bacterial pathogens are capable of exploiting and diverting host components such as  
94 proteoglycans for their pathogenesis (Aquino et al., 2018). These assemblies of  
95 glycosaminoglycans (GAGs) chains fixed around a protein nucleus (Bartlett and Park,  
96 2010) are expressed constitutively on the cell surface, in intracellular compartments as  
97 well as in the extracellular matrix. They are known to act as receptors for pathogens in  
98 many cases of infection (Aquino et al., 2018); (Rajas et al., 2017); (Gagoski et al., 2015).  
99 Many pathogens – e.g. *Chlamydia trachomatis* with a biphasic life cycle like *E.*  
100 *ruminantium* – use GAGs as an initial anchor site of low affinity; this facilitates interaction  
101 with their respective secondary receptor allowing internalization but GAGs are sometimes  
102 also used as bridging molecules (Aquino et al., 2010). Thus, whether *E. ruminantium* uses  
103 GAGs as a portal of entry or any specific bacterial surface protein is unknown but essential  
104 for developing any anti-infective measures.

105 The outer membrane proteome study of *E. ruminantium* Gardel strain revealed that a  
106 hypothetical protein, the possible major ferric iron binding protein precursor the putative  
107 iron transporter ERGA\_CDS\_01230, is uniquely expressed in the outer-membrane fraction  
108 (Moumene et al., 2015). This protein was also shown to be O-glycosylated only in *E.*  
109 *ruminantium* (Marcelino et al. 2019). Moreover, homologous counterparts of this protein in  
110 other pathogenic species play a key role in bacterial survival within the host by scavenging  
111 iron from mammalian serum iron transport proteins (Brown et al., 2010). Interestingly, we  
112 previously showed that iron starvation induces expression of virulence factors such as type  
113 IV secretion genes (Moumene et al., 2017).

114 In this study, we show that ERGA\_CDS\_01230 (UniProt Q5FFA9, named herein Ape for  
115 Adhesion protein of Ehrlichia ruminantium,) is involved in the binding of *E. ruminantium* to  
116 bovine aortic endothelial cells (BAEC). In order to study whether Ape alone can mediate  
117 the invasion of host cells by adhering to endothelial cells membrane, we used latex beads  
118 coated with recombinant Ape. These beads covered with the protein adhered and seemed  
119 to enter endothelial cells similarly to what is observed with *E. ruminantium in vitro*  
120 (Moumene and Meyer, 2015). Subsequent investigation uncovered that rApe is a  
121 glycosylated protein that induces a strong humoral immune response in vaccinated goats  
122 making it a possible vaccine candidate.

123

## 124 **Methods**

### 125 **Synchronous culture**

126 *E. ruminantium* (strain Gardel) was propagated in BAEC in Baby Hamster Kidney (BHK-  
127 21) cell medium supplemented with 1% L-glutamine 200mM (Eurobio), 10% heat-  
128 inactivated fetal bovine serum (FBS, Thermofisher), 1% penicillin 10000UI/ streptomycin  
129 10000 µg (Eurobio), 1x amphotericin B (Sigma), 5% NaHCO<sub>3</sub> 5.5%, under 5% CO<sub>2</sub> at  
130 37°C modified from (Marcelino et al., 2019). The cell trypsinization (Trypsin-Versen,  
131 Eurobio) was carried out with a splitting ratio of ½ when monolayer reached 100%  
132 confluence. Synchronous infection of a new BAEC monolayer was obtained using a  
133 bacterial suspension previously harvested at 120 hpi by scraping the TC flask (TCF) and  
134 passing infected lysed cells through 18G and 26G needles before reinfection at a ratio of  
135 1/20 (Marcelino et al., 2005).

136

### 137 **Quantitative reverse transcription RT-PCR along bacterial cycle**

138 *E. ruminantium*-infected BAE cells were harvested for RNA extraction by trypsinization at  
139 24, 48, 72 and 96 hours post infection (hpi), centrifuged 1700 x g, 5 min at 4°C and by cell  
140 lysate scrapping at 120 hpi, centrifuged 20000 x g, 15 min at 4°C. All pellets were  
141 dissolved in 1 mL TRIZOL (Thermofisher), RNA was extracted following manufacturer's  
142 recommendations and eluted in 100 µL H<sub>2</sub>O RNase/DNase free. RNA was treated by  
143 Turbo DNase (Ambion) according to supplier's instructions and precipitated overnight at -  
144 20°C in 2.5 volume (v/v) cold absolute ethanol (Normapur), 1/10 volume of 3 M sodium  
145 acetate and 1 µL glycogen 10 mg/mL (Thermofisher). Pellet obtained by centrifugation  
146 15000 x g, 10 min, 4°C was washed with 1 mL 75% ethanol, air dried after centrifugation

147 9000 x g, 7 min, 4°C and dissolved in 20 µL H<sub>2</sub>O RNase/ DNase free. Two µg ARN were  
148 reverse transcribed using "SuperScript™ VILO™ cDNA Synthesis Kit" (Invitrogen),  
149 according to the supplier's specifications.

150 Quantification started by 15 cycles of pre-amplification (same reaction mix and cycling  
151 conditions as below). ERGA\_CDS\_01230 (Ape) was amplified in 25 µL reaction mix  
152 containing 250 nM of the forward ERGA\_CDS\_01230F AATGGAGAATGAGGGGGAAG  
153 and reverse ERGA\_CDS\_01230R ACCCAAACCAAATCCATCA primers, 12.5 µL of  
154 Power SYBR® Green PCR Master Mix (Thermofisher), 12.5 µL H<sub>2</sub>O RNase/ DNase free  
155 and 20 µL pre-amplified DNA. Reactions were performed in a Quantstudio 5  
156 (Thermofisher) as follow: 50°C, 2 min for Uracil-N-Glycosylase activation, 95°C, 10 min for  
157 Uracil-N-Glycosylase inactivation and polymerase activation; 40 cycles 95°C, 15 sec  
158 denaturation and 59°C, 60 sec hybridization and elongation. The specificity of the PCR  
159 product was confirmed by the dissociation curves.

160 *E. ruminantium* quantification for normalization as described by (Pruneau et al., 2012), was  
161 performed by DNA extraction according to manufacturer's specifications (QiaAmp DNA  
162 minikit, QIAGEN, Courtaboeuf) on 1/10 of the harvested volume, after 20000 x g, 15 min  
163 centrifugation and dissolution in 200 µL PBS 1x, followed by a qPCR *Sol1* targeting the  
164 pCS20 region (Cangi et al., 2017). Normalization by *E. ruminantium* quantification was  
165 calculated:  $Rx_{hpi} = [cDNA\ copy\ number_{(ERGA\_CDS\_01230)}] / [E.\ ruminantium\ DNA\ copy$   
166  $number_{(pCS20)}]$ , allowing fold change (FC) determination, compared to expression at 96 hpi  
167 (corresponding to the stationnary phase of the bacterial growth):  $FC = R_{x\ hpi} / R_{96\ hpi}$ .  
168 Results were represented in log<sub>2</sub>, according to Pruneau et al. (2012) and confirmed by 2  
169 others kinetics (data not shown).

170

### 171 **Recombinant protein production**

172 pLEXY\_I-blecherry3 plasmid (Jena Bioscience, Germany) and 400 ng of amplified  
173 CDS\_ERGA\_01230 were digested 10 min at 37°C by BamHI and Sall (Thermo Scientific,  
174 USA) and column purified (Macherey Nagel, Germany). The digested product was ligated  
175 in pLEXY\_I-blecherry3 plasmid using T4 DNA Ligase (Thermo Scientific) for 1 h at 22°C.  
176 pLEXY\_I-blecherry3 plasmid was modified with the addition of a sequence coding GFP  
177 at C-terminus of the insert and 6X His tags at N-terminus of insert. It is to note that, GFP  
178 and the coding sequence of CDS\_ERGA\_01230 were linked with the sequence encoding  
179 cleavage site for Xa factor. Ligated plasmid was column purified and 50 ng of the ligation  
180 mix was electro-transferred to competent bacteria *E. coli* XL10 (Miller and Nickoloff, 1995).

181 100  $\mu$ L of transformed culture were spread on LB medium Petri dish supplemented with  
182 carbenicillin (50 $\mu$ g/ml). To confirm the presence of the plasmid and the insert, a PCR was  
183 performed on a colony using vector specific primers (Forward,  
184 CGCATCACCATCACCATCACG; Reverse, ACCAAAATTGGGACAACACCGTG). PCR  
185 product was then sequenced. Transformed E. coli clone was grown 16 h at 37°C under  
186 200 rpm stirring until optical density (OD) reached 3. The plasmid was isolated  
187 using “GenElute™ Plasmid Midiprep” kit (Sigma Aldrich) and digested with *Sma*I (Thermo  
188 Scientific)

189 *Leishmania tarentolae* preculture was grown in 10 mL LEXSY BHI medium with TC flask at  
190 26°C. 3 days after, preculture was diluted 10 fold in 10 mL LEXSY BHI medium and  
191 incubated overnight at 26°C (flat position). Next day, *Leishmania tarentolae* were  
192 centrifuged 5 min ( 2000 x g) and half of the medium was removed. Cells were  
193 resuspended in remaining medium to get 10<sup>8</sup> cells/ mL and incubated 10 min on ice. 350  
194  $\mu$ L cells were electroporated at 450 V, 450  $\mu$ F, 5 - 6 msec impulses with 5  $\mu$ g linearized  
195 plasmid (*sma*I digested). Cells were immediately incubated for 10 min on ice, transfer to  
196 10 mL LEXSY BHI medium (Bioscience) and incubated overnight. 10  $\mu$ L bleomycin (100  
197 mg/mL, Jena Bioscience) was then added to nonclonal selection for 3 more days. 5 mL of  
198 culture supernatant was centrifuged for 3 min at 1000 x g. Pellet was resuspended in 10  
199 mL LEXSY BHI medium containing bleomycin and incubated at 26°C for 5 days. After  
200 nonclonal selection, expression of protein was induced in 45 mL BHI medium  
201 supplemented with bleomycin and tetracyclin 10 mg/mL (Jena Bioscience). 5 ml of culture  
202 from nonclonal selection was added incubated for 72 h at 26°C with shaking at 100 rpm.  
203 Supernatant was harvested and concentrated in dialyses bag (3.5 kDa membrane, Serva)  
204 in a polyethylene glycol solution 20000 overnight at 4°C. Proteins were concentrated and  
205 purified by Sephadex gel filtration. Protein size was verified by MALDI TOF (Microflex,  
206 Bruker). The presence of GFP tag and associated fluorescence was checked respectively  
207 by immunoblotting and aggregation on Probond beads followed by fluorescence  
208 microscopy. Mass spectrometry allowed to check rApe size.

209

### 210 **3D Structure and localization prediction**

211 Protein structure prediction was accomplished using I-TASSER (Yang and Zhang, 2015)  
212 and view was generated by MacPyMol (DeLano, 2009). The subcellular localization was  
213 predicted by “CELLO 2.5: subCELLular LOcalization predictor” (Yu et al., 2006), from the

214 protein sequence, accession number CAI27575.1. Ape structural homology was  
215 determined using "Swiss model, Expasy" (Waterhouse et al., 2018).

216

### 217 **Western Blot for O-GlcNac Glycoprotein detection**

218 rApe was migrated on an acrylamide gel "SDS page" (NuPAGE bis-tris, Novex) for 2 h 30  
219 min at 100V and 400mA in MOPS buffer (Novex), according to the supplier's instructions  
220 (Nu PAGE Technical Guide). Approximately 10 µg protein were denatured at 70°C for 10  
221 min with LDS buffer and reducing agent (Novex) and migrated with a 3-198 kDa molecular  
222 weight marker (SeeBlue plus 2, Invitrogen). A gel-sized PVDF membrane (Amersham,  
223 Hybond-P) was soaked for 30 sec in methanol (Normapur) and incubated in transfer buffer  
224 (20x, NuPAGE) for at least 15 min with the same size filter papers (Whatman) and 4  
225 sponges. The transfer assembly was performed according to the NuPAGE technical guide  
226 and the transfer was run 1 h 15 min at 30 V, 170 mA. The membrane was then immersed  
227 in a solution of Culvert Red (AMRESCO) ~1 min and rinsed with water prior to picture. The  
228 protocol for western blot detection was modified from (Marcelino et al., 2019).The  
229 membrane was blocked for 3 h at room temperature (RT) with stirring in PBS (pH 7.4),  
230 0.05% Tween20 (PBS-T) and 5% milk. Then, membrane was incubated overnight with  
231 anti-O-GlcNAc antibody (Santa Cruz) diluted 200 fold in blocking solution. After three  
232 washes with PBS-T, membrane was incubated with anti-mouse antibody (IgM-HRP,  
233 Molecular probes) diluted 1000 fold in PBS-T for one hour. The membrane was washed 3  
234 times 10 min with PBS-T before the addition of the TMB substrate (Pierce) and gel reader  
235 picture once the color was developed.

236

### 237 **Glycosaminoglycans degradation assays**

238 10, 5, 1 and 0.3 µg/ mL heparan sulfate (Jonquieres et al., 2001;Kobayashi et al., 2010)  
239 and 9 µg/ mL rApe (positive control) were adsorbed in 50 µL of carbonate/bicarbonate  
240 buffer pH 9.6 (Martinez et al., 1993), distributed in Nunc Maxisorp wells, 1 h at 37°C with  
241 gentle stirring then overnight at 4°C. The next day, 3 washes were carried out with 200 µL  
242 of PBS-T per well. Blocking was done 1 h at 37°C under agitation with 100 µL of blocking  
243 buffer PBS tween 20 0.05% milk 3%, followed by 3 washes with 200 µL of PBS-T per well.  
244 50 µL/ well of rApe at 14.3 µg/mL diluted in PBS tween 20 0.05% milk 3% was incubated 1  
245 h at 37°C with stirring. Three washes of 200 µL PBS-T per well were performed, followed  
246 by addition of 50 µL anti-GFP antibody diluted to 4,000 in PBS-T with milk 3% and  
247 incubation 1 h at 37°C with stirring. Washings were repeated as above. Addition of 200 µL



248 TMB substrate allowed revelation within 30 min at 37°C before to stop the reaction with  
249 100 µL of H<sub>2</sub>SO<sub>4</sub> 2N. The reading was done at 450 nm (Multiskan, Thermofisher). 2 cm<sup>2</sup>  
250 wells were inoculated with ~1.1x10<sup>4</sup> BAEC in 500 µL BHK21 medium. When confluence  
251 was reached, several concentrations of chondroitinase were tested as follows: 0.2U, 0.4U  
252 and 0.9U/ mL chondroitinase was incubated 2 h before infection with the BAEC in 1X PBS  
253 and bovine fetal serum (SBF)-free BHK21 medium (Sava et al., 2009;Rajas et al., 2017).  
254 The medium was renewed with standard BKH21 prior infection at a ratio 1/20 and 2 h after  
255 infection. At lysis stage, all the wells were scraped, centrifuged for 15 min at 20,000 x g.  
256 DNA was extracted using the QiaAmp DNA minikit (Qiagen) and quantified using qPCR<sup>TM</sup>  
257 Sol1, targeting the pCS20 region (Cangi et al., 2017). The results were treated using the  
258  $\Delta\Delta C_t$  method and represented in  $2^{-\Delta\Delta C_t}$ .

259

#### 260 **Flow cytometry for attachment quantification**

261 We used the cytometer to quantify the fluorescence-labelled cells following incubation with  
262 rApe. Six-well Nunc plates (9.6 cm<sup>2</sup>/ well) with confluent BAEC were incubated for 2 h at  
263 37°C, 5% CO<sub>2</sub> with rApe concentrations ranging from 6.4 to 102.4 µg/ mL following the  
264 principle described in Lundberg et al., 2003. The negative control consisted of confluent  
265 BAE cells. After incubation with recombinant protein, each well was rinsed twice with 1 mL  
266 of 1X PBS and 1.5 mL of 1X PBS was used to scrape the well. After centrifugation during  
267 10 min at 200 x g, at 4°C cells were resuspended in Isoflow (Beckman) for further reading  
268 the percentage of fluorescent labelled cells on the cytometer (FC500, Beckman Coulter).

269

#### 270 **Far Western Blot**

271 The BHK21 culture medium of a 175 cm<sup>2</sup> TCF was removed, the TCF was washed with  
272 5mL of PBS 1x containing anti-protease (Roche). ~10mL of cold PBS 1x was added to  
273 gently scrap the cell mat. Centrifugation 10 min at 200 x g and 4°C was performed to  
274 remove the supernatant. Lysis of the pellet was performed by addition of 3 mL native lysis  
275 buffer (150 mM NaCl, 50 mM Tris-HCl, pH 7.4, NP-40 1%, anti-proteases 1%), followed by  
276 4 "freeze/thaw" cycles by first immersing the lysate 2 min in an ethanol/ ice bath, then 2  
277 min in a 37°C water bath. The lysate was vortexed between each bath. The cells were  
278 broken by passing the lysate 4 times through an 18G needle with a syringe. The cell debris  
279 were pelleted at 10000 x g for 30 min prior to supernatant transfer into a new tube.

280 Four different fractions (F1, cytosol components; F2, membrane and organelle  
281 components; F3, nucleus components; F4, the cytoskeleton) were extracted using the

282 "ProteoExtract Subcellular Proteome Extraction kit" (Calbiochem/ MERCK) according to  
283 the supplier's instructions. Each fraction was placed in acetone (at least 5x the volume of  
284 the extracted fraction) for overnight precipitation at -20°C. The day after, each pellet was  
285 re-suspended in 500µL of native lysis buffer after 20 min centrifugation at 15000 x g and  
286 4°C.

287 18 µL of each cell fraction and 35 µL of lysate were migrated onto acrylamide gel, with  
288 addition of LDS, under the same conditions as for the glycosylation tests (but without  
289 addition of reducing agent or heating), as well as for the transfer onto PVDF membrane.

290 The membrane was stored in TTBS 1x (10mM TRIS, 150mM NaCl, 0.05% Tween 20, pH  
291 8,3), then blocked for 1 h at RT under gentle agitation in 2% Bovine Serum Albumine  
292 (BSA) in TTBS and finally rinsed 3 times for 5 min with TTBS. The membrane was  
293 incubated overnight at 4°C under slow rotation with 0.5 mg rApe in 1% BSA in TTBS. The  
294 negative control (without recombinant protein) was incubated in the same conditions. The  
295 next day, the membrane was washed 3x for 5 min with TTBS and incubated 1 h at RT  
296 under agitation with anti-GFP-HRP (Thermofisher) diluted 2,500 fold in 1% BSA in TTBS.  
297 The membrane was washed again 3 x for 5 min with TTBS. The binding of anti- GFP-HRP  
298 was revealed by the addition of 4.5 mL peroxide substrate (Pierce Thermofisher) + 0.5mL  
299 chromogen DAB (Thermofisher) and incubation 10 min at RT. Picture was taken by  
300 colorimetry reading.

301

### 302 **Scanning electronic microscopy for binding assays**

303 Two kinds of fluorescent latex beads (with a sulfate group) were adsorbed with rApe  
304 through electrostatic interactions based on (Martinez et al., 2014). A total of  $10^{10}$  beads  
305 (0.1 µm in diameter) and  $7 \times 10^9$  beads (0.5 µm in diameter) were adsorbed with 100 µg/mL  
306 rApe in 1 mL of 25 mM MES, pH 6.1 (Sigma Aldrich) during 4h at RT under slow rotation.  
307 Then, three washes were performed using the same buffer before to be resuspended in 1  
308 mL of 1% BSA MES. 24-well plates containing 13 mm diameter lamellae (VWR) were  
309 inoculated with BAEC. A deposit of 0.1 or 0.5 µm-diameter beads ( $1.82 \times 10^8$  per well) was  
310 made in BHK21 medium. The negative control consisted of recombinant protein-free  
311 beads incubated with BAEC. The plate was centrifuged 5 min at 200 x g at RT before  
312 incubation 30-120 min at 37°C under 5% CO<sub>2</sub> atmosphere. Three washes with PBS 1X  
313 removed the excess of unbound beads before overnight fixation with 2%  
314 paraformaldehyde. Lamellae were then removed from each well and dehydrated in series

315 of acetone solutions of increasing concentration, dried to critical point in CO<sub>2</sub> and sputter-  
316 coated with gold before observation with a FEI Quanta 250 electron microscope at 20 kV.

317

### 318 **ELISA-based binding assays**

319 The antibody response to Ape during vaccination of goats was tested by ELISA. Sera for  
320 vaccinated goats obtained from previous studies (Marcelino et al. 2015 a, b) were  
321 incubated in wells coated with rApe, followed by incubation with anti-goat antibody coupled  
322 to HRP.

323 The adsorption of four µg/ mL rApe diluted in 100 µL of carbonate bicarbonate buffer pH  
324 9.6 was performed in a Nunc plate (Maxisorp). One hour incubation was carried out at  
325 37°C with stirring at 150 rpm then overnight at 4°C. The plate was washed with 300 µL/  
326 well of wash buffer (PBS 1x pH 7.2, Tween 20 0.1%). Blocking was carried out at 37°C  
327 with stirring in 300 µL blocking buffer (PBS1x, tween 20 0.1%, casein 2%) for 1 h.  
328 Washings were repeated as described in the previous step. 100 µL of each goat serum  
329 diluted 100-fold in blocking buffer was incubated 1 h at 37°C with agitation (Perez et al.,  
330 1998); 2 blank wells were incubated with 100 µL blocking buffer. Five washes with Wash  
331 Buffer preceded the deposit of 100 µL of anti-goat antibody (Rockland) diluted 20,000-fold  
332 in blocking buffer and 1 h incubation at 37°C with agitation. Five washes were performed.  
333 The revelation was performed by addition of 100 µL of TMB (Neogen) and stopping of the  
334 reaction after 5 min development by the addition of 50 µL of 0.5 M H<sub>2</sub>SO<sub>4</sub>. Antibody  
335 response was detected by ELISA titers and optical density (OD) was read with a  
336 spectrophotometer at 450nm. The OD of the wells without serum were valid when < 0.1 ;  
337 OD of negative samples were valid when < 0.2.

338

### 339 **Results**

340

#### 341 **ERGA\_CDS\_01230 (*ape*) is highly expressed at infectious elementary body stages** 342 **of *E. ruminantium* development inside mammalian cells**

343 In order to measure the expression of the *ape* gene, normalization was carried out in  
344 relation to the number of bacteria present at each stage of development since no  
345 reference gene with a sufficiently stable expression is available for *E. ruminantium*. The  
346 development cycle of *E. ruminantium* is synchronized when the lysis occurs 5 days after  
347 BAEC infection. Quantification of the number of bacteria present in the BAEC every 24 hpi  
348 by qPCR Sol1 showed a sigmoidal curve represented in log<sub>10</sub> (Figure 1A). The bacterium

349 had a slow growth phase between 24 and 48 hpi then an exponential development with a  
350 slowing down of the growth, a stationary phase after 96 hpi and a maximum of copies  
351 reached at 120 h (release of elementary bodies). The number of transcripts was  
352 determined by qPCR and a ratio calculated at each time as follow: (*E. ruminantium* <sub>cDNA</sub>  
353 number) / (*E. ruminantium* <sub>DNA copy</sub> number). The fold change (FC) was determined in relation to  
354 bacterial expression at 96 hpi (stationary phase) and represented graphically in Figure  
355 1B. The expression of *ape* gene peaks at the elementary body infectious stages of *E.*  
356 *ruminantium* life cycle which correspond to 120 hpi (host cell lysis) and 24 hpi (lag phase).  
357 These data indicate that *ape* is expressed when the bacterium is released and ready to  
358 infect new cells.

359

### 360 **Ape presents a C-clamp structure and is predicted to be an outer-membrane protein**

361 The 3D structure proposed by I-TASSER software (Figure 2A) showed that Ape harbours  
362 a succession of helices  $\alpha$  linked by loops distributed around a  $\beta$  sheet and showed a "c-  
363 clamp" three-dimensional structure. By homology with other known I<sup>ry</sup>, II<sup>ry</sup> or III<sup>ry</sup> structures,  
364 "Swiss model" showed a strong analogy of Ape with a "C-clamp" structure, capable of  
365 binding iron. According to the "CELLO 2.5" software, Ape has a dominant cytoplasmic  
366 localization (score of 2.418) but is also present at the outer membrane (1.652) (Figure 2B).  
367 This canonical sub-cellular localization of a transmembrane protein is in accordance with  
368 previous results finding this protein in the outer membrane proteome (Moumene et al.,  
369 2015).

370

### 371 **rApe shows O-glycosylated post-traductional modifications**

372 Western blot analysis showed that rApe was detected with an anti-O-GlcNAc antibody at  
373 the expected size of 66kDa (Figure 3). This size confirmed the data obtained by mass  
374 spectrometry and is 30% larger than the one estimated by the amino acid sequence  
375 encoded by *ape* gene (41 kDa for 365 amino acids). Altogether these results demonstrate  
376 the O-glycosylation of rApe.

377

### 378 **Enzymatic treatment of BAEC with chondroitinase decreases invasion by *E.*** 379 ***ruminantium***

380 To investigate whether GAGs have a role in *E. ruminantium* adhesion process, BAEC  
381 were treated with chondroitinase and then infected with *E. ruminantium*. The number of  
382 bacteria was calculated at the end of growth, during the lysis of the BAEC, by qPCR Sol1

383 for each treatment. After treatment with chondroitinase at 0.2U/mL, the FC corresponding  
384 to the bacterial amount differential was higher than for the condition without treatment but  
385 this may be explained by inter-well variability (Figure 4). Increasing chondroitinase  
386 concentrations to 0.4 and 0.9U/mL resulted in FC of 0.52 and 0.58, respectively,  
387 corresponding to a 50% reduction of the number of bacteria compared to the untreated  
388 condition, highlighting the role of chondroitin sulfate and dermatan sulfate in adhesion of  
389 *E. ruminantium* to the cell. No affinity of rApe for heparan sulfate could be revealed using  
390 HRP anti-GFP antibody (data not shown).

391

### 392 **rApe binds to BAEC**

393 To go further in the understanding of the role of Ape in *Ehrlichia ruminantium* invasion of  
394 host cells, we analyzed the interaction of rApe with the surface of endothelial cells using  
395 flow cytometry. Adhesion of recombinant proteins to BAEC was measured using flow  
396 cytometry to detect the fluorescence of rApe harboring GFP tag. The dot plot profile clearly  
397 showed that the percentage of labelled BAEC with rApe increases with the amount of rApe  
398 protein (Figure 5). As a negative control, the auto-fluorescence of the cells was measured  
399 on cells without recombinant protein incubation. The percentage of labelled cells increased  
400 with protein concentration up to 36 µg, showing a dose-effect relationship. Above these  
401 concentrations, saturation occurred with 50% of rApe labelled BAE.

402

### 403 **Ape interacts with BAEC lysate, membrane and organelles cell fractions**

404 The Far Western blot shows the interaction between rApe and the cell fractions as well as  
405 the lysate of the BAEC. rApe interacted with proteins of the cell lysate and more  
406 specifically with those of the membrane and organelle fraction (Figure 6).

407

### 408 **rApe coated beads adhere to BAEC and start internalization mechanism**

409 The visualization of interaction between rApe and the host cell was possible through usage  
410 of beads adsorbed with rApe (mimicking *Ehrlichia ruminantium*) and incubated with BAEC.  
411 Adhesion was evaluated by scanning electron microscopy. The negative control showed  
412 that non-coated beads did not adhere to the surface of the BAEC, that harbor their  
413 classical fried egg shape (Figure 7A). In contrast, Figure 7B showed swollen BAEC, dotted  
414 with rApe adsorbed beads after 30 minutes incubation, revealing an interaction between  
415 rApe and the BAEC. Figure 7C displayed that rApe-coated beads also adhere (black  
416 arrow) and begin to be invaginated (white arrow) by the endothelial cell membrane. Beads

417 diameter did not affect interaction of rApe and the BAEC. The images shown are  
418 representative of the observations made in other fields. These data reinforcing the results  
419 obtained by immunoblotting and flow cytometry prove that Ape interacts with the host cell  
420 membrane and is involved in the adhesion of *E. ruminantium* to the host cell.

421

### 422 **Ape induces an antibody response in vaccinated goats**

423 In order to verify if *E. ruminantium* Ape protein induces a humoral response following  
424 vaccination in goats, we tested sera from *in vivo* experiments on animals vaccinated with  
425 an inactivated or attenuated bacterial vaccine (Marcelino et al. 2015 a, b). Goats #614 and  
426 #915 were both naïve prior to vaccination, characterized by the absence of antibodies  
427 against Ape at 3 and 5 weeks post-vaccination, respectively (Figure 8). For #915, the  
428 ELISA test showed an increase in humoral response against rApe over time. In fact, the  
429 antibody response was developing between 5 and 7 weeks post-vaccination, the latter  
430 corresponding to the vaccine boost. For goat #614, inoculation of an attenuated bacterial  
431 vaccine also conducted to a humoral response, including response against rApe.. These  
432 results suggest that rApe could be a relevant target for further studies to see whether it  
433 could be a protective immunogen in *E. ruminantium* infection *in vivo*.

434

### 435 **Discussion**

436 Controlled and determined *Ehrlichia* entry into host cell is a fundamental first step for an  
437 effective infectious developmental cycle, particularly for an obligate intracellular pathogen  
438 that strictly relies on its host to grow. In the last decade, comparative genomics and  
439 cellular microbiology allowed major discoveries in the molecular pathogenesis of  
440 *Anaplasmataceae*. These integrated approaches led to the effective identification of  
441 several bacterial virulence determinants (e.g. effectors and regulators) and their diverse  
442 mechanisms of action (Cheng et al., 2008; Rikihisa, 2017; Marcelino et al., 2015b ;  
443 Moumene et al., 2017; Noroy and Meyer, 2017; Noroy and Meyer, 2021). Notably, Rikihisa  
444 *et al.* identified that the EtpE protein governs the binding and entry of *E. chaffeensis* into its  
445 host cells (Mohan Kumar et al., 2013). The binding of EtpE to DNaseX elicits a signaling  
446 cascade that results in cytoskeleton modification, filopodial induction and finally  
447 endocytosis into the host cell (Green et al., 2020). Previous studies demonstrated that  
448 functional conservations of molecular pathogenicity determinants can occur between of *E.*  
449 *chaffeensis* and *E. ruminantium* (Moumene et al., 2017) but such bacterial ligand was still  
450 unknown in *E. ruminantium* at the beginning of this study. Among other *Rickettsiales*, a

451 receptor-mediated endocytosis was only reported for *Rickettsia conorii* (Moumene et al.,  
452 2017 ; Martinez et al., 2005).

453 Our aim being to determine some major pathogenicity determinants of *E. ruminantium*, we  
454 chose to analyze ERGA\_CDS\_01230 (Ape, UniProt Q5FFA9), a putative iron-transporter  
455 previously identified in the outer-membrane proteome of *E. ruminantium* (Moumene et al.,  
456 2015). Indeed, we postulated that some key bacterial proteins involved in the early  
457 interaction with the eukaryotic host cell should be overexpressed at early stages of the  
458 developmental cycle and at the bacterial-host interface. Moreover, we previously showed  
459 that iron was a triggering environmental cue for several *E. ruminantium* molecular  
460 virulence determinants. Indeed, iron depletion induced a master regulatory gene, genes  
461 encoding outer-membrane proteins of the Map1 family and genes of the Type IV Secretion  
462 System, a major bacterial pathogenicity determinant (Moumene et al., 2017). Therefore,  
463 taking into account that iron is a virulence triggering signal of *Ehrlichia*, Ape protein being a  
464 putative iron transporter made it an excellent candidate for further characterization. In the  
465 present study, we focused on the role of Ape protein in the interaction between *E.*  
466 *ruminantium* and its mammalian host cell, notably during adhesion. As depicted in our  
467 working model for *E. ruminantium* binding and invasion of its host endothelial cell (Figure  
468 9), we showed that Ape epitopes are recognized by the immune system of goats  
469 vaccinated with live attenuated strain or killed strain or *E. ruminantium*. Indeed, after  
470 vaccination, we detected Ape antibodies in sera of vaccinated goats indicating a global  
471 humoral response. Following this model, the initial binding of *E. ruminantium* onto the host  
472 cell surface seems to involve glycosaminoglycans (GAGs) as chondroitinase treatment of  
473 BAEC resulted in a significant decrease of the number of bacteria present at the end of  
474 development cycle. The *ape* gene is highly expressed at the elementary body  
475 developmental stages of *E. ruminantium*, particularly during host cell lysis which  
476 precedes *E. ruminantium* release from host cells to initiate a new cycle of infection.  
477 Interestingly, recombinant protein rApe is an O-glycosylated protein that interacts with cell  
478 membrane and latex beads coated with rApe were able to adhere to the BAEC surface to  
479 initiate internalization and follows a similar pattern of entry like that of *E. ruminantium*  
480 (Moumene and Meyer, 2015).

481 Our results showed that Ape protein, an *Ehrlichia* ligand different from previously identified  
482 *E. chaffeensis* EtpE (Mohan Kumar et al., 2013), is important for *E. ruminantium* adhesion  
483 to the mammalian host cells. The mechanisms used by *E. ruminantium* to invade its host  
484 are still not elucidated compared to other pathogens of the order *Rickettsiales*. Indeed

485 *Rickettsia conorii* uses OmpA (Hillman et al., 2013) to adhere to the host cell whereas two  
486 different receptors were described for *Anaplasma marginale* and *A. phagocytophilum*  
487 mobilizing Msp1a and OmpA (de la Fuente et al., 2003), (Hebert et al., 2017), Asp14 and  
488 OmpA (Kahlon et al., 2013), (Ojogun et al., 2012), respectively to attach cell membrane.  
489 Adhesins and invasins were largely described in other bacteria as surface located  
490 structures for specific interaction with host cell receptors (Niemann et al., 2004). *Yersinia*  
491 outer membrane invasin interacts with  $\beta$ 1 integrin receptors, inducing several reactions  
492 including actin rearrangements at the site of bacterial entry, promoting invasion.  
493 *Salmonella* translocates several effectors into target cells, some of them allowing the initial  
494 uptake of the bacterium, whereas *Listeria* uses InIA and InIB-dependent molecular  
495 pathways, (Pizarro-Cerda and Cossart, 2006). Ligands often show elongated molecules  
496 containing domains commonly found in eukaryotic proteins (Niemann et al., 2004).  
497 We showed that rApe is O-glycosylated. Post-translational modifications are one of the  
498 most important mechanisms for activating, changing, or suppressing protein functions,  
499 being widely used by pathogens to interact with their hosts. *E. ruminantium*  
500 glycoproteomics showed a high percentage of glycoproteins, many of them being O-  
501 glycosylated (Marcelino et al., 2019). *E. ruminantium* “mucin”, which is also glycosylated,  
502 was presented as an adhesin for tick cells, reinforcing a role of glycans in *Ehrlichia*  
503 adhesin molecules (de la Fuente et al., 2004). The strength of ligand-receptor bacterial  
504 interactions is optimized depending on their environment but weak enough to allow a  
505 bacterium to detach regularly and migrate to other locations (Formosa-Dague et al., 2018).  
506 Glycan-glycan interactions in bacterial-mammalian cells systems were characterized as  
507 low-affinity weak interactions preceding high-affinity protein-glycan or protein-protein  
508 interactions but recent studies have documented the importance of such interactions in  
509 bacterial adhesion (Formosa-Dague et al., 2018). Indeed, we determined that the  
510 presence GAG on the surface of BAE plays a key role in the attachment of *Ehrlichia* to  
511 bovine endothelial cells *in vitro*, reinforcing the hypothesis that several receptors are  
512 probably required in *E. ruminantium* adhesion and subsequent infection of host cells.  
513 Chondroitinase treatment significantly affected *Ehrlichia* entry compared to the untreated  
514 condition. The enzymatic digestion of chondroitin and dermatan from BAEC reduced the  
515 rate of infection of the BAEC, as *E. ruminantium* can no longer adhere to the surface of the  
516 cells. Indeed, in other models like Chlamydia, GAGs were shown to be used for initial  
517 attachment to host cells (Tiwari et al., 2012) ; Lyme disease *Borreliae* requires  
518 glycosaminoglycan binding activity to colonize and disseminate to tissues (Lin et al.,



519 2017). Even though heparan sulfate appears to be the most important GAG species  
520 involved in bacterial binding, both heparan sulfate and chondroitin sulfate were able to  
521 influence the attachment of mucoid *P. aeruginosa*, *H. influenza* and *B. cepacia* in specific  
522 ways that were dependent on the cell line involved (Martin et al., 2019). *Borrelia*  
523 *burgdorferi* has multiple surface proteins with different binding specificities to GAGs  
524 depending on the tissue affected (Leong et al., 1998). Different GAGs act as receptors for  
525 *B. burgdorferi* depending on the host cells; both heparin sulfate and heparan sulfate are  
526 essential in adherence to primary endothelium and adult kidney Vero cells, but only  
527 dermatan sulfate is involved in attachment to human embryonic kidney cells (Garcia et al.,  
528 2016).

529 Although we did not establish the interaction of rApe adhesion with a cellular receptor, we  
530 can still hypothesize that Ape actively triggers *Ehrlichia* internalization by the mean of a  
531 ligand/receptor interaction. Kumar *et al.* already suggested the existence of additional  
532 mammalian receptors for *Ehrlichia* infection (Mohan Kumar et al., 2013). The present  
533 study identified the bacterial of a putative second *Ehrlichia* invasion-receptor pair and  
534 highlights the importance of this molecular control of invasion for the *Anaplasmataceae*  
535 intracellular bacteria. The probable existence of several ligand-receptor systems could  
536 indeed serve the bacteria to infect a broader host range of animal reservoirs and vector  
537 ticks. Moreover, GAG degradation following chondroitinase treatment severely impaired  
538 *Ehrlichia* infection. This suggests that Ape could interact with a  
539 glycosylphosphatidylinositol (GPI)-anchored protein as previously shown for PSGL-1 that  
540 is required for the binding and infection of human HL-60 cells by *A. phagocytophylum*  
541 (Herron et al., 2000), This remains to be further studied as well as its role in iron uptake of  
542 *Ehrlichia ruminantium* (Reneer et al., 2008).

543 In summary, with the identification of Ape (ERGA\_CDS\_01230), we found the first  
544 *Ehrlichia ruminantium* protein that is involved in host cell invasion. Whether the *E.*  
545 *chaffeensis* EtpE homolog (ERGA\_CDS\_08340) is functional in *E. ruminantium* remain to  
546 be explored, but these outer-membrane proteins can now be considered as immune-  
547 dominant pathogen-associated molecular patterns (Budachetri et al., 2020). Our next step  
548 is now investigate the use of rApe as a new vaccine candidate against Heartwater. In light  
549 of the lack of prophylactic measures against *Ehrlichia* spp. and the rising appearance of  
550 antibiotic resistances, deep understanding of invasion mechanisms is of prime importance  
551 and will help to propose efficient alternative therapeutics blocking the early interaction  
552 between these obligate intracellular bacteria and their host cells.

553

554 **Acknowledgements and funding information**

555 The authors acknowledge the financial support from Franco-Slovak bilateral project PHC  
556 Stephanik 2014 n°31798XB and from European Union in the framework of the European  
557 Regional Development Fund (ERDF), n° 2015-FED-186, MALIN project “Surveillance,  
558 diagnosis, control and impact of infectious diseases of humans, animals and plants in  
559 tropical islands”. We also gratefully acknowledge Géraldine Bossard and Valérie  
560 Rodrigues for technical assistance in the development of ELISA assays.

## 561 References

- 562 Allsopp, B.A. (2010). Natural history of Ehrlichia ruminantium. *Vet Parasitol* 167, 123-135.
- 563 Aquino, R.S., Lee, E.S., and Park, P.W. (2010). Diverse functions of glycosaminoglycans in infectious diseases. *Prog*  
564 *Mol Biol Transl Sci* 93, 373-394.
- 565 Aquino, R.S., Teng, Y.H., and Park, P.W. (2018). Glycobiology of syndecan-1 in bacterial infections. *Biochem Soc*  
566 *Trans*.
- 567 Bartlett, A.H., and Park, P.W. (2010). Proteoglycans in host-pathogen interactions: molecular mechanisms and  
568 therapeutic implications. *Expert Rev Mol Med* 12, e5.
- 569 Bioscience, J. (2011). LEXSInduce 3 Expression Kit for inducible expression of recombinant proteins in *Leishmania*  
570 *tarentolae*. 28.
- 571 Brown, R.N., Romine, M.F., Schepmoes, A.A., Smith, R.D., and Lipton, M.S. (2010). Mapping the subcellular  
572 proteome of *Shewanella oneidensis* MR-1 using sarkosyl-based fractionation and LC-MS/MS protein  
573 identification. *J Proteome Res* 9, 4454-4463.
- 574 Budachetri, K., Teymournejad, O., Lin, M., Yan, Q., Mestres-Villanueva, M., Brock, G.N., and Rikihisa, Y. (2020). An  
575 Entry-Triggering Protein of Ehrlichia Is a New Vaccine Candidate against Tick-Borne Human Monocytic  
576 Ehrlichiosis. *mBio* 11.
- 577 Cangi, N., Gordon, J.L., Bournez, L., Pinarello, V., Aprelon, R., Huber, K., Lefrancois, T., Neves, L., Meyer, D.F., and  
578 Vachieri, N. (2016). Recombination Is a Major Driving Force of Genetic Diversity in the Anaplasmataceae  
579 Ehrlichia ruminantium. *Front Cell Infect Microbiol* 6, 111.
- 580 Cangi, N., Pinarello, V., Bournez, L., Lefrancois, T., Albina, E., Neves, L., and Vachieri, N. (2017). Efficient high-  
581 throughput molecular method to detect *Ehrlichia ruminantium* in ticks. *Parasit Vectors* 10, 566.
- 582 Cheng, Z., Wang, X., and Rikihisa, Y. (2008). Regulation of type IV secretion apparatus genes during Ehrlichia  
583 chaffeensis intracellular development by a previously unidentified protein. *J Bacteriol* 190, 2096-2105.
- 584 De La Fuente, J., Garcia-Garcia, J.C., Barbet, A.F., Blouin, E.F., and Kocan, K.M. (2004). Adhesion of outer membrane  
585 proteins containing tandem repeats of *Anaplasma* and *Ehrlichia* species (Rickettsiales: *Anaplasmataceae*) to  
586 tick cells. *Vet Microbiol* 98, 313-322.
- 587 De La Fuente, J., Garcia-Garcia, J.C., Blouin, E.F., and Kocan, K.M. (2003). Characterization of the functional domain  
588 of major surface protein 1a involved in adhesion of the rickettsia *Anaplasma marginale* to host cells. *Vet*  
589 *Microbiol* 91, 265-283.
- 590 Deem, S.L. (1998). A review of heartwater and the threat of introduction of *Cowdria ruminantium* and *Amblyomma*  
591 spp. ticks to the American mainland. *J Zoo Wildl Med* 29, 109-113.
- 592 Delano, W.L. (2009). The PyMOL molecular graphics system.
- 593 Dumler, J.S., Barbet, A.F., Bekker, C.P., Dasch, G.A., Palmer, G.H., Ray, S.C., Rikihisa, Y., and Rurangirwa, F.R.  
594 (2001). Reorganization of genera in the families *Rickettsiaceae* and *Anaplasmataceae* in the order  
595 Rickettsiales: unification of some species of *Ehrlichia* with *Anaplasma*, *Cowdria* with *Ehrlichia* and *Ehrlichia*  
596 with *Neorickettsia*, descriptions of six new species combinations and designation of *Ehrlichia equi* and 'HGE  
597 agent' as subjective synonyms of *Ehrlichia phagocytophila*. *Int J Syst Evol Microbiol* 51, 2145-2165.
- 598 Formosa-Dague, C., Castelain, M., Martin-Yken, H., Dunker, K., Dague, E., and Sletmoen, M. (2018). The Role of  
599 Glycans in Bacterial Adhesion to Mucosal Surfaces: How Can Single-Molecule Techniques Advance Our  
600 Understanding? *Microorganisms* 6.
- 601 Frutos, R., Viari, A., Ferraz, C., Bensaid, A., Morgat, A., Boyer, F., Coissac, E., Vachieri, N., Demaille, J., and  
602 Martinez, D. (2006). Comparative genomics of three strains of *Ehrlichia ruminantium*: a review. *Ann N Y Acad*  
603 *Sci* 1081, 417-433.
- 604 Frutos, R., Viari, A., Vachieri, N., Boyer, F., and Martinez, D. (2007). Ehrlichia ruminantium: genomic and  
605 evolutionary features. *Trends Parasitol* 23, 414-419.
- 606 Gagoski, D., Mureev, S., Giles, N., Johnston, W., Dahmer-Heath, M., Skalamera, D., Gonda, T.J., and Alexandrov, K.  
607 (2015). Gateway-compatible vectors for high-throughput protein expression in pro- and eukaryotic cell-free  
608 systems. *J Biotechnol* 195, 1-7.
- 609 Gannon, F., Neilan, J., and Powell, R. (1988). Current Protocols in Molecular-Biology - Ausubel, Fm. *Nature* 333, 309-  
610 310.
- 611 Garcia, B., Merayo-Lloves, J., Martin, C., Alcalde, I., Quiros, L.M., and Vazquez, F. (2016). Surface Proteoglycans as  
612 Mediators in Bacterial Pathogens Infections. *Front Microbiol* 7, 220.
- 613 Green, R.S., Izac, J.R., Naimi, W.A., Obier, N., Breitschwerdt, E.B., Marconi, R.T., and Carlyon, J.A. (2020). Ehrlichia  
614 chaffeensis EplA Interaction With Host Cell Protein Disulfide Isomerase Promotes Infection. *Front Cell Infect*  
615 *Microbiol* 10, 500.
- 616 Hebert, K.S., Seidman, D., Oki, A.T., Izac, J., Emani, S., Oliver, L.D., Jr., Miller, D.P., Tegels, B.K., Kannagi, R.,  
617 Marconi, R.T., and Carlyon, J.A. (2017). Anaplasma marginale Outer Membrane Protein A Is an Adhesin That  
618 Recognizes Sialylated and Fucosylated Glycans and Functionally Depends on an Essential Binding Domain.  
619 *Infect Immun* 85.

- 620 Herron, M.J., Nelson, C.M., Larson, J., Snapp, K.R., Kansas, G.S., and Goodman, J.L. (2000). Intracellular parasitism  
621 by the human granulocytic ehrlichiosis bacterium through the P-selectin ligand, PSGL-1. *Science* 288, 1653-  
622 1656.
- 623 Hillman, R.D., Baktash, Y.M., and Martinez, J.J. (2013). OmpA-mediated rickettsial adherence to and invasion of  
624 human endothelial cells is dependent upon interaction with alpha2beta1 integrin. *Cell Microbiol* 15, 727-741.
- 625 Jonquieres, R., Pizarro-Cerda, J., and Cossart, P. (2001). Synergy between the N- and C-terminal domains of InlB for  
626 efficient invasion of non-phagocytic cells by *Listeria monocytogenes*. *Mol Microbiol* 42, 955-965.
- 627 Kahlon, A., Ojogun, N., Ragland, S.A., Seidman, D., Troese, M.J., Ottens, A.K., Mastronunzio, J.E., Truchan, H.K.,  
628 Walker, N.J., Borjesson, D.L., Fikrig, E., and Carlyon, J.A. (2013). *Anaplasma phagocytophilum* Asp14 is an  
629 invasin that interacts with mammalian host cells via its C terminus to facilitate infection. *Infect Immun* 81, 65-  
630 79.
- 631 Kasari, J.R., Miller, R.S., James, A.M., and Freier, J.E. (2010). Recognition of the threat of *Ehrlichia*  
632 *ruminantium* infection in domestic and wild ruminants in the continental United States. *Journal of the*  
633 *American Veterinary Medical Association* 2010 237:5, 520-530. <https://doi.org/10.2460/javma.237.5.520>
- 634 Kobayashi, K., Kato, K., Sugi, T., Takemae, H., Pandey, K., Gong, H., Tohya, Y., and Akashi, H. (2010). *Plasmodium*  
635 *falciparum* BAEBL binds to heparan sulfate proteoglycans on the human erythrocyte surface. *J Biol Chem*  
636 285, 1716-1725.
- 637 Leong, J.M., Robbins, D., Rosenfeld, L., Lahiri, B., and Parveen, N. (1998). Structural requirements for  
638 glycosaminoglycan recognition by the Lyme disease spirochete, *Borrelia burgdorferi*. *Infect Immun* 66, 6045-  
639 6048.
- 640 Lin, M., Liu, H., Xiong, Q., Niu, H., Cheng, Z., Yamamoto, A., and Rikihisa, Y. (2016). *Ehrlichia* secretes Etf-1 to  
641 induce autophagy and capture nutrients for its growth through RAB5 and class III phosphatidylinositol 3-  
642 kinase. *Autophagy* 12, 2145-2166.
- 643 Lin, Y.P., Li, L., Zhang, F., and Linhardt, R.J. (2017). *Borrelia burgdorferi* glycosaminoglycan-binding proteins: a  
644 potential target for new therapeutics against Lyme disease. *Microbiology* 163, 1759-1766.
- 645 Lundberg, M., Wikstrom, S., and Johansson, M. (2003). Cell surface adherence and endocytosis of protein transduction  
646 domains. *Mol Ther* 8, 143-150.
- 647 Marcelino, I., Colome-Calls, N., Holzmüller, P., Lisacek, F., Reynaud, Y., Canals, F., and Vachieri, N. (2019). Sweet  
648 and Sour Ehrlichia: Glycoproteomics and Phosphoproteomics Reveal New Players in *Ehrlichia ruminantium*  
649 Physiology and Pathogenesis. *Front Microbiol* 10, 450.
- 650 Marcelino, I., Verissimo, C., Sousa, M.F., Carrondo, M.J., and Alves, P.M. (2005). Characterization of *Ehrlichia*  
651 *ruminantium* replication and release kinetics in endothelial cell cultures. *Vet Microbiol* 110, 87-96.
- 652 Marcelino I, Lefrançois T, Martinez D, Giraud-Girard K, Aprelon R, Mandonnet N, Gaucheron J, Bertrand F, Vachiéry  
653 N. (2015a) A user-friendly and scalable process to prepare a ready-to-use inactivated vaccine: the example of  
654 heartwater in ruminants under tropical conditions. *Vaccine*. 29;33(5):678-85. doi:  
655 10.1016/j.vaccine.2014.11.059. Epub 2014 Dec 13. PMID: 25514207.
- 656 Marcelino I, Ventosa M, Pires E, Müller M, Lisacek F, et al. (2015b) Comparative Proteomic Profiling of *Ehrlichia*  
657 *ruminantium* Pathogenic Strain and Its High-Passaged Attenuated Strain Reveals Virulence and Attenuation-  
658 Associated Proteins. *PLOS ONE* 10(12): e0145328. <https://doi.org/10.1371/journal.pone.0145328>
- 659 Martin, C., Lozano-Iturbe, V., Giron, R.M., Vazquez-Espinosa, E., Rodriguez, D., Merayo-Lloves, J., Vazquez, F.,  
660 Quiros, L.M., and Garcia, B. (2019). Glycosaminoglycans are differentially involved in bacterial binding to  
661 healthy and cystic fibrosis lung cells. *J Cyst Fibros* 18, e19-e25.
- 662 Martinez, D., Coisne, S., Sheikboudou, C., and Jongejan, F. (1993). Detection of antibodies to *Cowdria ruminantium* in  
663 the serum of domestic ruminants by indirect ELISA. *Rev Elev Med Vet Pays Trop* 46, 115-120.
- 664 Martinez, E., Cantet, F., Fava, L., Norville, I., and Bonazzi, M. (2014). Identification of OmpA, a *Coxiella burnetii*  
665 protein involved in host cell invasion, by multi-phenotypic high-content screening. *PLoS Pathog* 10,  
666 e1004013.
- 667 Martinez, J.J., Seveau, S., Veiga, E., Matsuyama, S., and Cossart, P. (2005). Ku70, a component of DNA-dependent  
668 protein kinase, is a mammalian receptor for *Rickettsia conorii*. *Cell* 123, 1013-1023.
- 669 Miller, E.M., and Nickoloff, J.A. (1995). *Escherichia coli* electrotransformation. *Methods Mol Biol* 47, 105-113.
- 670 Mohan Kumar, D., Yamaguchi, M., Miura, K., Lin, M., Los, M., Coy, J.F., and Rikihisa, Y. (2013). *Ehrlichia*  
671 *chaffeensis* uses its surface protein EtpE to bind GPI-anchored protein DNase X and trigger entry into  
672 mammalian cells. *PLoS Pathog* 9, e1003666.
- 673 Moumene, A., Gonzalez-Rizzo, S., Lefrançois, T., Vachieri, N., and Meyer, D.F. (2017). Iron Starvation Conditions  
674 Upregulate *Ehrlichia ruminantium* Type IV Secretion System, trl Transcription Factor and map1 Genes  
675 Family through the Master Regulatory Protein ErxR. *Front Cell Infect Microbiol* 7, 535.
- 676 Moumene, A., Marcelino, I., Ventosa, M., Gros, O., Lefrançois, T., Vachieri, N., Meyer, D.F., and Coelho, A.V.  
677 (2015). Proteomic profiling of the outer membrane fraction of the obligate intracellular bacterial pathogen  
678 *Ehrlichia ruminantium*. *PLoS One* 10, e0116758.
- 679 Moumene, A., and Meyer, D.F. (2015). *Ehrlichia's* molecular tricks to manipulate their host cells. *Microbes Infect*.

- 680 Niemann, H.H., Schubert, W.D., and Heinz, D.W. (2004). Adhesins and invasins of pathogenic bacteria: a structural  
681 view. *Microbes Infect* 6, 101-112.
- 682 Noroy, C., Lefrancois, T., and Meyer, D.F. (2019). Searching algorithm for Type IV effector proteins (S4TE) 2.0:  
683 Improved tools for Type IV effector prediction, analysis and comparison in proteobacteria. *PLoS Comput Biol*  
684 15, e1006847.
- 685 Noroy, C., and Meyer, D.F. (2017). Comparative Genomics of the Zoonotic Pathogen *Ehrlichia chaffeensis* Reveals  
686 Candidate Type IV Effectors and Putative Host Cell Targets. *Front Cell Infect Microbiol* 7, 120.
- 687 Noroy, C., and Meyer, D.F. (2021). The super repertoire of type IV effectors in the pangenome of *Ehrlichia* spp.  
688 provides insights into host-specificity and pathogenesis. *PLoS Comput Biol*. 10.1371/journal.pcbi.1008788
- 689 Ojogun, N., Kahlon, A., Ragland, S.A., Troese, M.J., Mastronunzio, J.E., Walker, N.J., Viebrock, L., Thomas, R.J.,  
690 Borjesson, D.L., Fikrig, E., and Carlyon, J.A. (2012). *Anaplasma phagocytophilum* outer membrane protein A  
691 interacts with sialylated glycoproteins to promote infection of mammalian host cells. *Infect Immun* 80, 3748-  
692 3760.
- 693 Perez, J.M., Martinez, D., Sheikboudou, C., Jongejan, F., and Bensaid, A. (1998). Characterization of variable  
694 immunodominant antigens of *Cowdria ruminantium* by ELISA and immunoblots. *Parasite Immunol* 20, 613-  
695 622.
- 696 Pizarro-Cerda, J., and Cossart, P. (2006). Bacterial adhesion and entry into host cells. *Cell* 124, 715-727.
- 697 Pruneau, L., Emboule, L., Gely, P., Marcelino, I., Mari, B., Pinarello, V., Sheikboudou, C., Martinez, D., Daigle, F.,  
698 Lefrancois, T., Meyer, D.F., and Vachieri, N. (2012). Global gene expression profiling of *Ehrlichia*  
699 *ruminantium* at different stages of development. *FEMS Immunol Med Microbiol* 64, 66-73.
- 700 Rajas, O., Quiros, L.M., Ortega, M., Vazquez-Espinosa, E., Merayo-Lloves, J., Vazquez, F., and Garcia, B. (2017).  
701 Glycosaminoglycans are involved in bacterial adherence to lung cells. *BMC Infect Dis* 17, 319.
- 702 Reneer, D.V., Troese, M.J., Huang, B., Kearns, S.A., and Carlyon, J.A. (2008). *Anaplasma phagocytophilum* PSGL-1-  
703 independent infection does not require Syk and leads to less efficient AnkA delivery. *Cell Microbiol* 10, 1827-  
704 1838.
- 705 Rikihisa, Y. (2017). Role and Function of the Type IV Secretion System in *Anaplasma* and *Ehrlichia* Species. *Curr Top*  
706 *Microbiol Immunol* 413, 297-321.
- 707 Sava, I.G., Zhang, F., Toma, I., Theilacker, C., Li, B., Baumert, T.F., Holst, O., Linhardt, R.J., and Huebner, J. (2009).  
708 Novel interactions of glycosaminoglycans and bacterial glycolipids mediate binding of enterococci to human  
709 cells. *J Biol Chem* 284, 18194-18201.
- 710 Teymournejad, O., Lin, M., and Rikihisa, Y. (2017). *Ehrlichia chaffeensis* and Its Invasin EtpE Block Reactive Oxygen  
711 Species Generation by Macrophages in a DNase X-Dependent Manner. *mBio* 8.
- 712 Tiwari, V., Maus, E., Sigar, I.M., Ramsey, K.H., and Shukla, D. (2012). Role of heparan sulfate in sexually transmitted  
713 infections. *Glycobiology* 22, 1402-1412.
- 714 Truttmann, M.C., Rhomberg, T.A., and Dehio, C. (2011). Combined action of the type IV secretion effector proteins  
715 BepC and BepF promotes invasome formation of *Bartonella henselae* on endothelial and epithelial cells. *Cell*  
716 *Microbiol* 13, 284-299.
- 717 Waterhouse, A., Bertoni, M., Bienert, S., Studer, G., Tauriello, G., Gumienny, R., Heer, F.T., De Beer, T.a.P., Rempfer,  
718 C., Bordoli, L., Lepore, R., and Schwede, T. (2018). SWISS-MODEL: homology modelling of protein  
719 structures and complexes. *Nucleic Acids Res* 46, W296-W303.
- 720 Yan, Q., Lin, M., Huang, W., Teymournejad, O., Johnson, J.M., Hays, F.A., Liang, Z., Li, G., and Rikihisa, Y. (2018).  
721 *Ehrlichia* type IV secretion system effector Etf-2 binds to active RAB5 and delays endosome maturation. *Proc*  
722 *Natl Acad Sci U S A* 115, E8977-E8986.
- 723 Yang, J., and Zhang, Y. (2015). I-TASSER server: new development for protein structure and function predictions.  
724 *Nucleic Acids Res* 43, W174-181.
- 725 Yu, C.S., Chen, Y.C., Lu, C.H., and Hwang, J.K. (2006). Prediction of protein subcellular localization. *Proteins* 64,  
726 643-651.
- 727

728 **Figure captions**

729 **Figure 1. Temporal expression of the (ERGA\_CDS\_01230) *ape* gene in *E.***  
730 ***ruminantium* determined by qRT-PCR.**

731 (A) *E. ruminantium* sigmoidal growth curve was determined by qPCR targeting *pCS20*  
732 region and represented as log 10 along the cycle of development

733 (B) Transcript levels were determined from 24, 48, 72 and 120 hpi by qRT-PCR targeting  
734 ERGA\_CDS\_01230 gene. Levels were normalized by the quantity of bacteria measured  
735 by qPCR *Sol1* and the ratio was compared to 96 hpi, allowing fold-change (FC)  
736 determination, expressed as log 2. Values at each time point are the means +/- standard  
737 deviations for 2 biological replicates. Gp38 is for *E. ruminantium* Gardel strain, passage  
738 #38 (virulent strain).

739

740 **Figure 2. Structural characterization of Ape protein.**

741 (A) I-TASSER derived prediction of the ERGA\_CDS\_01230 gene product. Ape shows a  
742 succession of  $\alpha$  helices linked by loops distributed around a  $\beta$  sheet, organized as a three-  
743 dimensional “c-clamp” structure.

744 (B) Reliability score prediction by CELLO 2.5 software of the subcellular localization of the  
745 native *E. ruminantium* Ape protein. Ape presents a typical subcellular localization of an  
746 active transporter, with a dominant cytoplasmic localization and is also present at the outer  
747 membrane.

748

749 **Figure 3. rApe is an O-glycosylated recombinant protein.**

750 Composite picture of a Western blot detecting O-glycosylation of recombinant Ape protein  
751 (lane 2). Recombinant proteins were separated by SDS-PAGE, then transferred to PVDF  
752 and incubated with anti-O-GlcNAc antibody. The Western blot was probed with anti-mouse  
753 IgM-HRP antibody and revealed by TMB substrate. Lane 1: negative control; lane 2: rApe.  
754 Numbers and black arrowheads indicate molecular masses in kilodaltons (kDa). The  
755 recognized rApe is significantly larger (66 kDa) than the one predicted by the amino acid  
756 sequences encoded by ERGA\_CDS\_01230 gene (41 kDa).

757

758 **Figure 4. Chondroitinase impairs BAEC infection by *E. ruminantium*.** Using 0.4 and  
759 0.9U/mL chondroitinase resulted in a halving of the number of bacteria compared to the  
760 untreated condition. Bacterial quantification was performed at lysis stage by qPCR *sol1*  
761 after chondroitinase treatment at three different concentration. Fold-change (FC) was

762 obtained by calculating the bacterial amount differential for each condition compared to the  
763 condition without treatment and represented as  $2^{-\Delta\Delta Ct}$ .

764

765 **Figure 5. rApe attaches to the host cells.**

766 Different concentrations of rApe tagged with GFP were incubated with BAEC. Adherence  
767 of GFP-rApe to prefixed BAEC was evaluated by flow cytometry and showed a dose-effect  
768 relationship up to 36  $\mu\text{g}$  of rApe. Fluorescent-labelled cells quantified by flow cytometry are  
769 represented in % for each concentration point. Auto-fluorescence was evaluated with cells  
770 without recombinant protein.

771

772 **Figure 6. rApe interacts with cell lysate and membrane fractions.**

773 Composite picture of a Far-Western blot detecting Ape protein. Lysate and cell fractions  
774 were separated by SDS-PAGE, transferred to PVDF and incubated either with rApe (left  
775 panel) or PBS as a negative control (right panel). The Western blot was probed with rabbit  
776 anti-GFP-HRP antibody, and revealed by peroxide substrate mixed with chromogen DAB.  
777 1: protein ladder, 2 and 5: cell lysate, 3: cytoskeleton fraction, 4 and 6: membrane and  
778 organelles fraction.

779

780 **Figure 7. rApe is sufficient for adhesion of latex beads to bovine endothelial cells.**

781 Representative images of BAEC incubated 30 minutes with fluorescent latex beads  
782 ( $1.82 \times 10^8$ ) coated with rApe and processed for scanning electron microscopy.

783 (A) Endothelial cells did not retain non-adsorbed beads ( $0.1 \mu\text{m}$  diameter) on their cell  
784 surface. (B) On the opposite, the whole surface of the same type of cells are covered with  
785 adherent beads ( $0.5 \mu\text{m}$  diameter) absorbed with rApe. (C) Enlarged view of adherent  
786 beads. Such beads present two kinds of localizations. Some of them are already  
787 internalized (black arrow heads) while others are still located outside the cell remaining in  
788 contact with the cytoplasmic membrane (white arrow heads). Scale bars are indicated.

789

790 **Figure 8. Ape induces an antibody response in sera of vaccinated goats.**

791 The antibody response to Ape during vaccination kinetic was tested by ELISA. Sera of  
792 vaccinated goats were incubated in wells coated with rApe, followed by incubation with  
793 anti-goat antibody coupled to HRP. Antibody response was detected by ELISA titers  
794 (optical density at 450 nm). Shown are representative results from five vaccinated goats.

795 #614: goat vaccinated with an attenuated vaccine. #915: goat vaccinated with an

796 inactivated vaccine. The time (in weeks) post-vaccination is indicated. Goats vaccinated  
797 with inactivated vaccine were also challenged for resistance to *E. ruminantium* Gardel  
798 strain seven weeks post vaccination.

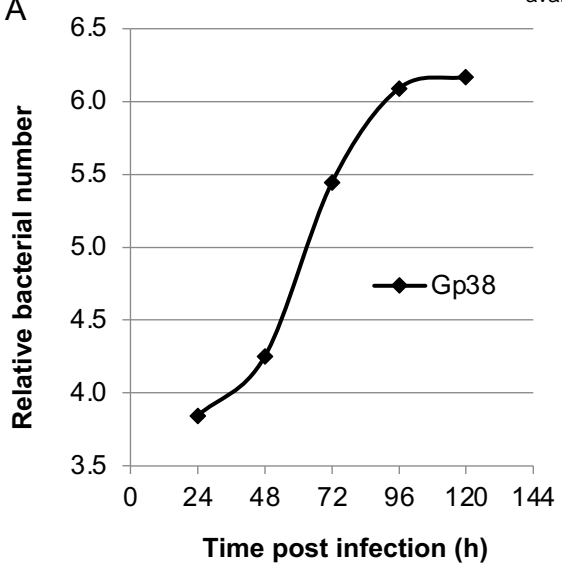
799

800 **Figure 9. Schematic representation of *Ehrlichia ruminantium* binding to mammalian**  
801 **cells and rApe interaction with the host cell surface.**

802 Ape is located at *E. ruminantium* outer membrane and is recognized by antibody from sera  
803 of vaccinated animals. *E. ruminantium* can adhere and enter into BAEC but infection is  
804 reduced when GAG like chondroitin and dermatan sulfate are degraded. The recombinant  
805 version of *E. ruminantium*, rApe, is glycosylated and latex beads coated with rApe bind to  
806 BAE cell surface and start to enter in BAEC, in a similar manner that of *E. ruminantium*.  
807 Whether Ape binds to a cellular receptor and the following triggered signaling cascade  
808 remain to be determined.



A



B

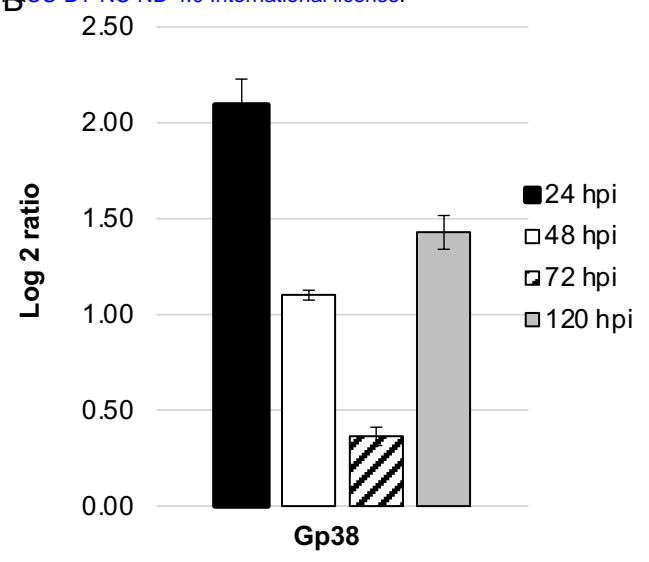
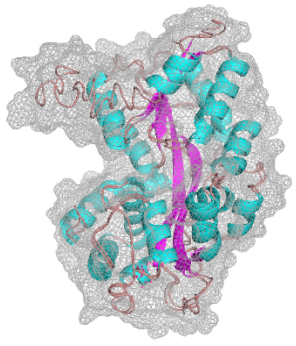


Figure 1



A

| <b>BACTERIAL LOCALIZATION</b> | <b>ERGA_CDS_01230</b> |
|-------------------------------|-----------------------|
| Cytoplasmic                   | <b>2,418</b>          |
| Outer membrane                | <b>1,652</b>          |
| Periplasmic                   | 0,424                 |
| Inner membrane                | 0,404                 |
| Extracellular                 | 0,102                 |

B

Figure 2

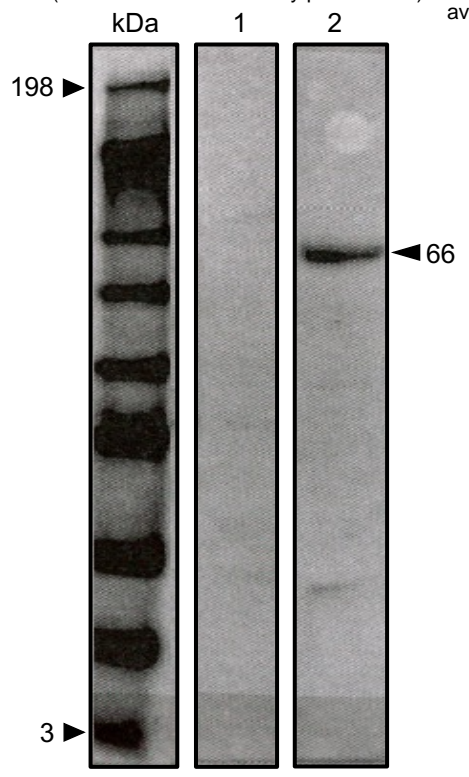


Figure 3

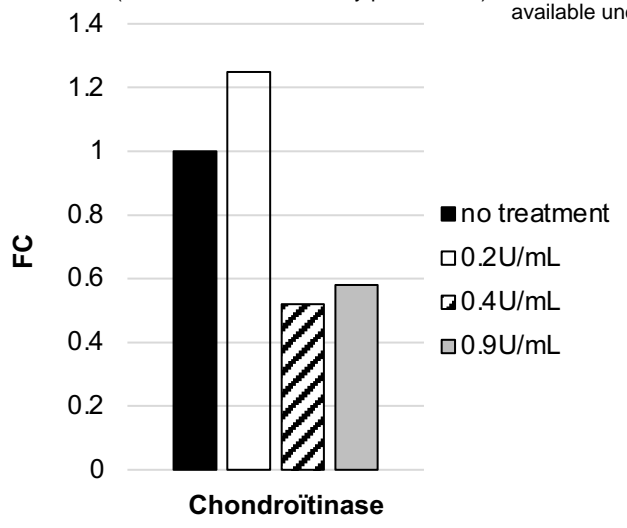


Figure 4

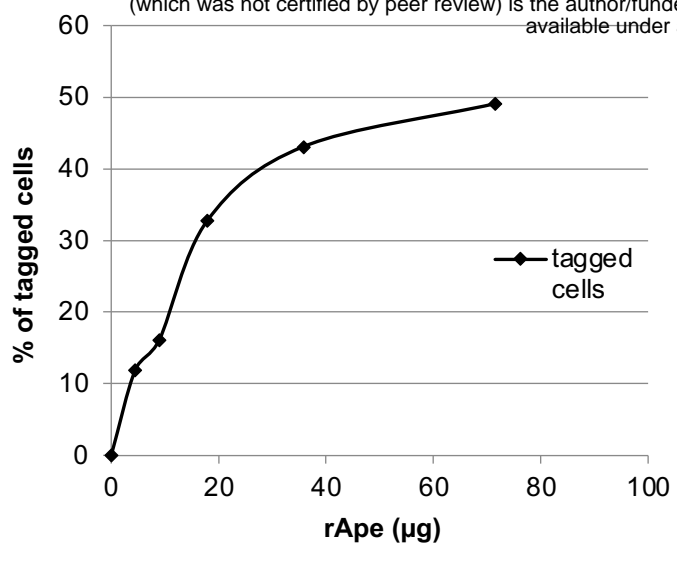


Figure 5

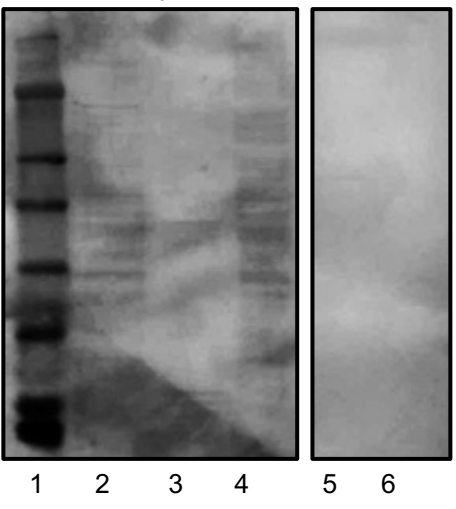


Figure 6

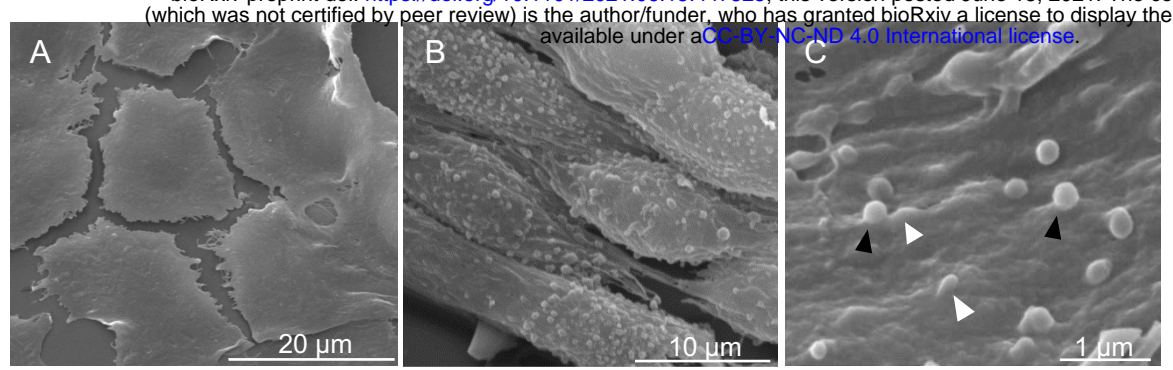


Figure 7

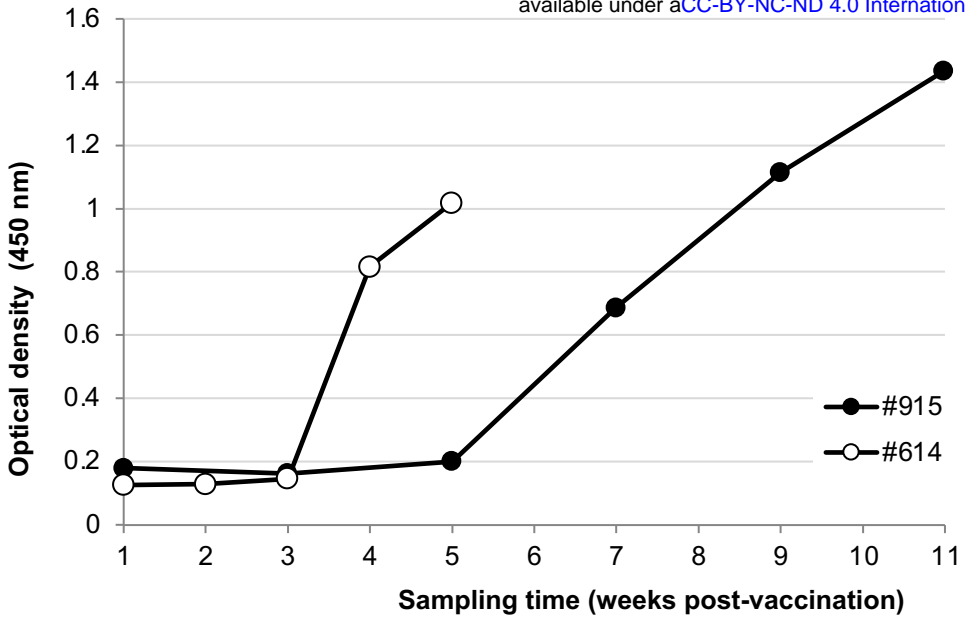


Figure 8



